Letters in Applied NanoBioScience
Open-Access Journal (ISSN: 2284-6808)

Article
Volume 15, Issue 2, 2026, 75
https://doi.org/10.33263/LIANBS152.075

Computational Evaluation of Neem-Derived Compounds as FTO Inhibitors for Metabolic Disorder Therapy

Selvaraj Sathyapriya [1], Chaitanya Sree Somala [2], Mohamed Adil [2], Nagaraj Bharathkumar [2], Renganathan Senthil [3], Konda Mani Saravanan [4,*], Thirunavukarasou Anand [5,*]

1 Faculty of Clinical Research, Sri Ramachandra Institute of Higher Education and Research, Chennai, Tamil Nadu, 600116, India; g.s.sathyapriya@gmail.com (S.S.); anand.sriic@gmail.com (T.A.);
2 B-Aatral Biosciences Private Limited, Bangalore, Karnataka, 560091, India; schaitu27@gmail.com (C.S.S.); adilmdaa@gmail.com (M.A.); bharathkumarbcas@gmail.com (N.B.);
3 Department of Bioinformatics, School of Lifesciences, Vels Institute of Science Technology and Advanced Studies (VISTAS), Pallavaram, Chennai 600117, Tamil Nadu, India; rsenthil.sls@vistas.ac.in;
4 Center for Research Impact & Outcome, Chitkara College of Pharmacy, Chitkara University, Rajpura, Punjab, 140401, India; saravananbioinform@gmail.com;
5 Department of Cell Biology & Molecular Genetics, Sri Devaraj Urs Academy of Higher Education and Research (Deemed to be University), Kolar, Karnataka, 563103, India; anandarasou28@gmail.com;
* Correspondence: saravananbioinform@gmail.com (K.M.S.); ; anandarasou28@gmail.com (T.A.);
Received: 13.02.2025; Accepted: 24.02.2026; Published: 30.06.2026

Abstract: The study of fat mass and obesity-associated (FTO) enzymes holds promise for managing metabolic disorders and preventing cancer growth. Neem-derived compounds have shown potential as natural inhibitors of FTO. This study aimed to evaluate the effectiveness of neem-derived chemicals as FTO inhibitors by analyzing their electronic properties, drug-like characteristics, and molecular interactions. Molecular docking simulations were performed to assess the binding affinity of neem-derived compounds with FTO. Drug-likeness was evaluated using Lipinski's rule of five, and electronic properties were analyzed using HOMO-LUMO energy gaps. Quercetin exhibited the strongest binding affinity (-7.80 kcal/mol) and the most thermodynamically stable binding free energy (-45.749 kcal/mol) due to stabilizing interactions with active site residues HIS320, ARG316, LEU203, and SER229. Nimbidol (-7.70 kcal/mol), Nimbidin (-7.50 kcal/mol), and Gedunin (-7.40 kcal/mol) also demonstrated inhibitory potential. Drug-likeness assessments showed that all compounds, except Azadirachtin, met pharmacokinetic suitability criteria. The significant HOMO-LUMO energy gap in quercetin indicated high molecular stability, reinforcing its potential as a promising drug-like molecule. Neem-derived compounds, especially quercetin, may act as FTO inhibitors and could be developed into plant-based treatments for metabolic disorders, though further biological testing is needed.

Keywords: FTO protein; molecular docking; quercetin; metabolic diseases; natural compounds.

1. Introduction

Obesity and the metabolic disorders that come with it are seen as big global health problems in the 21st century because they have a negative effect on health rates and death rates [1–3]. Cancer is still one of the leading causes of death in the world, even though it is so difficult that it requires advanced therapeutic interventions [4–6]. A recent study shows that the Fat Mass and Obesity-Associated (FTO) protein is an important regulator of both metabolic

disorders and tumor growth [7]. Because it alters RNA stability and splicing, the RNA demethylase FTO acts as an RNA regulator by altering m6A modifications [8,9]. Researchers have found that problems with the FTO protein can cause cells to malfunction by increasing adipogenesis, altering metabolism, and promoting the growth of cancer cells [10]. FTO is a plausible therapeutic goal that holds hope for treating diseases linked to obesity as well as cancer growth [11]. The therapeutic potential of targeting FTO in obesity and cancer suggests that investigating natural compounds, particularly those derived from medicinal plants such as neem, is a viable approach to discovering effective FTO inhibitors.

Researchers are exploring natural compounds as potential sources of new drugs due to their bioactive therapeutic properties [12–14]. To design new drugs, scientists use compounds from plants because they are bioavailable and easy to synthesize [15]. Neem (Azadirachta indica), a medicinal plant, has been the subject of research due to its diverse healing properties, including the ability to kill microbes, reduce inflammation, fight cancer, and help people with diabetes [16]. Neem's medicinal effects come from its secondary metabolites, which include terpenoids, flavonoids, and polyphenols. These have a lot of influence on changing different biological targets [17]. Because FTO is a drug target with well-established therapeutic properties, the study focuses on whether compounds from neem can inhibit it. There is a potential new way to control RNA demethylation pathways that use natural compounds that bind to FTO. This can help treat metabolic conditions and the biological processes of cancer. Combining molecular docking methods with drug-likeness predictions provides an effective way to identify FTO-specific compounds with strong binding properties [18].

According to a previous study, neem bioactive compounds have shown promise in inhibiting several molecular processes linked to disease [19]. The current study uses *in silico* methods to assess how well important neem compounds bind to the FTO protein and the drug properties they exhibit. The main goal of this study is to progress in developing FTO-targeting plant-based drugs. *In silico* methods are being used along with old traditional information about neem to find new possible drug compounds that could change how advanced obesity, cancer, and metabolic disorders are treated.

2. Materials and Methods

2.1. Protein target.

The study examines the crystal structure of the FTO protein bound by the control compounds (3-methylthymidine ligand, N-oxalylglycine), and Fe(II) ion conditions [8,20,21]. The X-ray diffraction examination of the crystal structure enabled researchers to ascertain it at a resolution of 2.75 Å, recorded under Protein Data Bank identifier 3LFM. The 495-amino acid protein comprises two distinct domains: an amino-terminal domain associated with AlkB proteins and a carboxy-terminal region exhibiting a unique folding configuration. The jelly-roll motif of FTO exhibits structural distinctiveness due to a distinctive loop that spans the preserved pattern.

2.2. Ligands.

Eight bioactive compounds derived from Neem (Azadirachta indica) were selected as ligands to investigate their binding affinities to the FTO protein in this investigation. The study utilized eight bioactive chemicals from neem (Azadirachta indica) as ligands: Quercetin, Nimbidol, Nimbidin, Gedunin, Azadirachtin, Nimbin, Nimbolinin, and Salannin [22]. A subset

of these neem compounds was selected based on evidence of their anti-inflammatory, antioxidant, and anticancer properties, as well as their role in regulating metabolic and enzymatic pathways [23]. The polyphenolic flavonoid quercetin was selected for its potent antioxidant properties and established ability to interact with proteins that regulate metabolic pathways. The selection of Nimbidol, Nimbidin, and Nimbin was based on their demonstrated anti-inflammatory and antibacterial properties, which may be advantageous in treating metabolic disorders [24]. Gedunin and Azadirachtin were selected for their antiparasitic and anticancer properties, which interact with critical proteins and influence cellular processes [25–27]. The researchers investigated the FTO protein's structural and functional activities in conjunction with Nimbolinin and Salannin due to these substances' recognized immunomodulatory and antioxidant capabilities [28].

The researchers selected compounds from neem due to their diverse biological roles, which may facilitate the development of medicinal treatments for metabolic illnesses [29]. The natural compounds exhibit low toxicity, making them promising candidates for drug discovery research [30]. Their unique chemical structures allow researchers to investigate novel binding interactions with the FTO protein, which regulates RNA demethylation and metabolism. The research objective evaluates the capacity of these ligands to regulate FTO activity, as this assessment may facilitate novel plant-derived medicinal discoveries.

2.3. Protein and ligand preparation.

The present investigation utilized the FTO protein crystal structure (PDB ID: 3LFM) obtained from the Protein Data Bank [31]. The structural determination using X-ray diffraction techniques to achieve a resolution of 2.75 Å, elucidating critical information on the active site and co-factor Fe(II) ions within the protein [20]. Before docking calculations, AutoDockTools (v1.5.7) removed water molecules, heteroatoms, and all non-essential ligands from the protein structure [32]. FTO necessitates the Fe(II) ion for catalytic function, and the active site effectively preserves this crucial element. Swiss-PDBViewer was utilized to build missing residues, and the energy minimization was conducted using the AMBER14 force field to stabilize the protein structure [33]. The PDBQT-formatted structure of the prepared protein was used for docking experiments, following the identification of active-site residues via literature review and structural analysis.

The study assessed eight compounds sourced from the PubChem database, specifically Quercetin, Nimbidol, Nimbidin, Gedunin, Azadirachtin, Nimbin, Nimbolinin, and Salannin, along with their 2D structures [34,35]. The structures of neem compounds were converted to 3D using Open Babel, and energy minimization was performed with the MMFF94 force field to obtain the most energetically stable conformations [36]. AutoDockTools facilitated the construction of each ligand by specifying rotatable bonds before saving them in PDBQT format.

2.4. Drug likeness prediction.

The assessment of drug-likeness for neem-derived chemicals was conducted utilizing the SwissADME web-based prediction platform (www.swissadme.ch) for pharmacokinetic characteristics and drug-likeness evaluation [37]. SwissADME obtained SMILES (Simplified Molecular Input Line Entry System) notations from PubChem to assess drug-likeness characteristics, which encompassed molecular weight, logP lipophilicity, hydrogen bond

donors (HBD), hydrogen bond acceptors (HBA), and the count of rotatable bonds. An evaluation based on Lipinski's Rule of Five was conducted to predict the oral bioavailability of the drug. The pharmacokinetic properties of the compounds were assessed using filters derived from the Ghose, Veber, Egan, and Muegge criteria. The study performed ADMET analysis to identify drugs exhibiting favorable bioavailability and low toxicity potential.

2.5. HOMO LUMO gap calculation.

The HOMO-LUMO (Highest Occupied Molecular Orbital - Lowest Unoccupied Molecular Orbital) energy gap (ΔE) serves as a stability indicator and a reactivity measure for chemical compounds among the selected neem-derived compounds. The reactivity levels of compounds increase as ΔE values decrease, but larger ΔE values indicate compounds that are more resistant to change. The research used Avogadro (v1.2) for molecular geometry optimization using MMFF94 force-field calculations, followed by PM6 semi-empirical methods in ORCA or Firefly quantum chemical analysis tools [38]. The analysis of the electronic behavior and binding efficiency potential of compounds relied on determining HOMO and LUMO energy levels and evaluating the ΔE values.

2.6. Molecular docking.

AutoDock Vina software was used for performing molecular docking of FTO protein binding interactions with eight different neem-derived compounds [39]. Despite keeping the essential Fe(II) ion necessary for FTO activity, the protein structure was optimized by removing water molecules and non-essential ligands. Before saving the structure in PDBQT format, the structure was subjected to optimization using AutoDockTools (v1.5.7) to include polar hydrogens and Kollman charges. To get the ligands ready, we used PubChem to obtain their 2D structures, then Open Babel and the MMFF94 force field to convert them to 3D. For ligands saved in PDBQT format, the AutoDockTools (v1.5.7) program defined rotatable bonds.

The grid box definition applied to the FTO active site captured key residues, the Fe(II) ion, and other important components. The docking grid was centered at coordinates (X = 34.5, Y = 27.2, Z = 45.8) with dimensions of 30 × 30 × 30 Å, which sufficiently encompassed the active site of the FTO protein, including the Fe(II) ion and surrounding catalytic residues. The docking procedure produced multiple binding conformations for each ligand using AutoDock Vina. To illustrate the ranking binding poses from the AutoDock Vina results, the docking study used PyMOL and Chimera [40,41]. It also showed hydrophobic contacts and hydrogen bonds.

2.8. Binding free energy calculations.

To study how strongly the FTO protein binds to neem-derived ligands, the open-source g_mmpbsa software was used to run MM/PBSA calculations linked to GROMACS (v2021.5) [42,43]. The top docking poses from AutoDock Vina were used as starting points for energy minimization in GROMACS using the AMBER99SB force field. An MD simulation that lasted between 2 and 5 ns took place in a solvated system that contained water. The SPC/E water model was used as the solvent, and 0.15 M NaCl was added to keep the system neutral [44]. The g_mmpbsa tool calculated van der Waals, electrostatic, polar, and nonpolar solvation energies, and binding free energy components along the MD trajectories. An average value from the stable simulation period was used to determine the binding free energy. This gave us

quantitative information about how the molecules interacted. The system used open-source tools like GROMACS and g_mmpbsa to do accurate, cost-effective calculations of binding affinities for testing ligands derived from neem as FTO inhibitors.

3. Results and Discussion

3.1. Structural chemistry of protein and ligands.

Figure 1 shows the FTO protein's structure in Panel A and the chemical structures of compounds from neem in Panels B through I. Panel A shows the three-dimensional structure of the FTO protein. Its secondary elements are shown, comprising α-helices (red) and β-sheets (cyan). Together, they form a jelly-roll shape. A clear sphere shows the active site of the protein in the figure. The sphere shows green levels indicating important binding sites that enable ligand docking and catalytic reactions. For demethylase function, the exact structure and folding of the FTO protein are needed for Fe(II) ions to bind to substrate molecules [20].

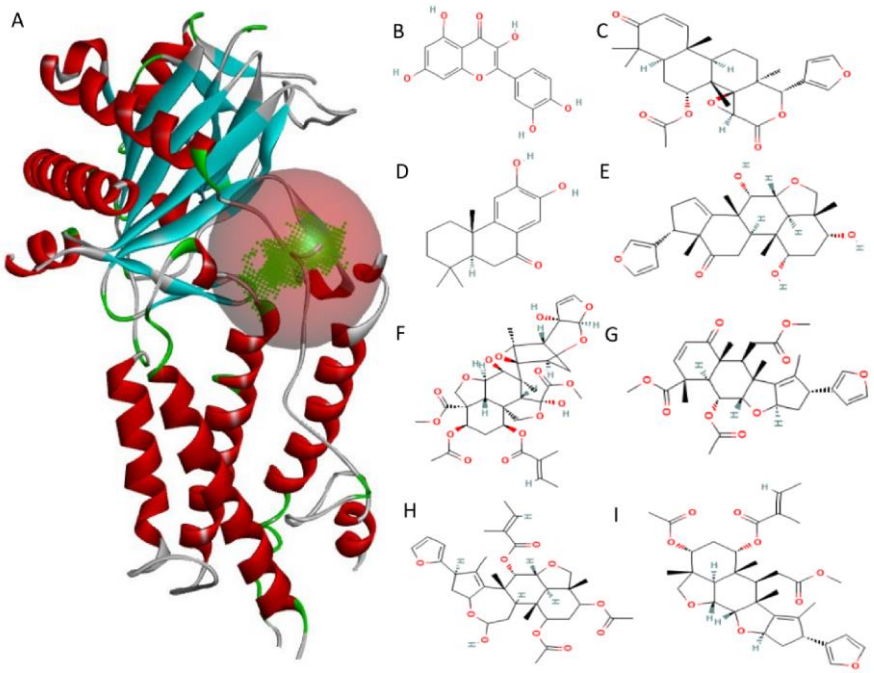

Figure 1. Structural representation of the FTO protein and neem-derived ligands. **(A)** Three-dimensional structure of the FTO protein (PDB ID: 3LFM) highlighting α-helices (red), β-sheets (cyan), and loops (grey). The active site is indicated by a transparent sphere, with green density representing the binding pocket critical for ligand interaction. (B–I) Chemical structures of neem-derived ligands used in the study: **(B)** Quercetin; **(C)** Nimbidol; **(D)** Nimbidin; **(E)** Gedunin; **(F)** Azadirachtin; **(G)** Nimbin; **(H)** Nimbolinin; **(I)** Salannin. Each ligand exhibits distinct functional groups and structural frameworks, showcasing the diversity of neem-derived compounds evaluated for binding to the FTO protein.

In panels B to I, two-dimensional sketches of eight neem-derived compounds are presented. Different functional groups and unique molecular arrangements make up neem compounds, influencing their pharmacological properties. The active-site residues of the FTO protein could form hydrogen bonds with the hydroxyl groups of planar quercetin. Panels C and D show the chemical structures of Nimbidol and Nimbidin. These terpenoid structures with hydroxyl groups could form hydrophobic and hydrogen bonds. Panels E through I show Neem limonoid structures like Gedunin, Azadirachtin, Nimbin, Nimbolinin, and Salannin. The chemical structures comprise joined rings, multiple oxygen moieties, and different stereochemical arrangements. Because these compounds have special building blocks, they can

associate with proteins in several ways, such as through metal coordination, van der Waals bonds, and hydrogen bonds [45].

3.2. Drug likeness properties of neem compounds.

The data in Table 1 show the physicochemical properties of neem-derived ligands, which show how similar they are to drugs. The bioavailability score of quercetin is 0.55, its synthetic accessibility score stays at 3.23, and its molecular weight stays at 302.24; it obeys Lipinski's rules. Also, Nimbidiol and Nimbidin exhibit favorable binding characteristics because they have low molecular weights (274.35 and 442.54, respectively) and no Lipinski violations [46]. They also have relatively synthetic accessibility scores. Gedunin's bioavailability score stays the same, and its molecular weight is 482.57. This is because it meets Lipinski's rules, which means it could be a good lead chemical [47].

Azadirachtin is not a good candidate for a drug because it has the highest molecular weight (720.71) and a lot of Lipinski violations. After all, it has a lot of high hydrogen bond acceptors (16) and donors (3), which means it is not bioavailable (0.17) and is very hard to synthesize (8.11). The possibility of developing drugs with Nimbin, Nimbolinin, and Salannin is limited because they have high molecular weights and synthetic accessibility scores. The neem compounds studied meet most of the criteria for drug-likeness, but their bioavailability scores differ. Azadirachtin is the only one that doesn't, with a score of 0.55. Most compounds have good solubility and permeability, which are associated with oral bioavailability, based on their TPSA values. They also exhibit balanced hydrophilicity and lipophilicity, as indicated by their LOGP values. The table shows that compounds derived from neem exhibit diverse shapes and levels of drug-likeness, making them highly valuable for discovering new FTO protein inhibitors that work well [18].

Table 1. Physicochemical and drug-likeness properties of neem-derived ligands. The table summarizes key properties of the selected ligands, including molecular weight (MW), rotatable bonds, hydrogen bond acceptors and donors, topological polar surface area (TPSA), partition coefficient (LOGP), Lipinski rule violations, bioavailability scores, and synthetic accessibility. These properties provide insights into the ligands' drug-likeness, pharmacokinetic potential, and ease of synthesis.

Molecule	MW	Rotatable bonds	H-bond acceptors	H-bond donors	TPSA	LOGP	Lipinski violations	Bioavailability score	Synthetic accessibility
Quercetin	302.24	1	7	5	131.36	1.63	0	0.55	3.23
Nimbidiol	274.35	0	3	2	57.53	2.14	0	0.55	3.13
Nimbidin	442.54	1	6	3	100.13	1.97	0	0.55	6.18
Gedunin	482.57	3	7	0	95.34	3.23	0	0.55	6.48
Azadirachtin	720.71	10	16	3	215.34	2.9	2	0.17	8.11
Nimbin	540.6	8	9	0	118.34	3.68	1	0.55	6.54
Nimbolinin	626.73	8	10	1	130.73	4.23	1	0.55	7.33
Salannin	596.71	9	9	0	110.5	3.61	1	0.55	7.04

3.3. HOMO LUMO energy.

The HOMO, LUMO, and HOMO-LUMO gap values in Table 2 show the electronic properties of compounds obtained from neem. These values affect both the stability and reactivity of molecules and chemicals. Azadirachtin and Nimbolinin have the largest HOMO-LUMO gap value, which is -0.449 eV. This means that they are more chemically stable than the other ligands. Nimbin has the smallest HOMO-LUMO gap reading, which is -0.393 eV. This means that the ligand may have better reactivity potential and the ability to connect to electrons [48]. The HOMO-LUMO gap range of Quercetin, Nimbidiol, Nimbidin, Gedunin,

and Salannin is between -0.400 and -0.446 eV, which means that these molecules are neither very stable nor very reactive.

Table 2. HOMO-LUMO energy levels and energy gaps of neem-derived ligands. The table presents the calculated Highest Occupied Molecular Orbital (HOMO), Lowest Unoccupied Molecular Orbital (LUMO), and HOMO-LUMO gap values for the neem-derived compounds. The HOMO-LUMO gap (ΔE) reflects the electronic stability and reactivity of the compounds, with smaller gaps indicating higher reactivity and larger gaps suggesting greater stability.

S.No	Compound Name	Compound ID	HOMO	LUMO	HOMO-LUMO Gap
1	Quercetin	CID_5280343	-0.319	0.081	-0.400
2	Nimbidiol	CID_11334829	-0.309	0.093	-0.402
3	Nimbidin	CID_101306757	-0.297	0.149	-0.446
4	Gedunin	CID_12004512	-0.329	0.095	-0.424
5	Azadirachtin	CID_5281303	-0.339	0.110	-0.449
6	Nimbin	CID_108058	-0.296	0.097	-0.393
7	Nimbolinin	CID_6440564	-0.302	0.148	-0.449
8	Salannin	CID_6437066	-0.303	0.116	-0.419

Azadirachtin and Gedunin are good at donating electrons because their HOMO values are very low (-0.339 eV and -0.329 eV, respectively). On the other hand, Quercetin and Nimbidiol are good at accepting electrons because their LUMO values are very low (0.081 eV and 0.093 eV, respectively). The active site of the FTO protein needs these electronic features to see how well ligands can interact with it by moving charges around or joining the Fe(II) ion. Figure 2 shows how ligands derived from neem spread their HOMO and LUMO properties. HOMO orbitals, which are shown by green regions and have electron-donating properties, are found next to LUMO orbitals, which are shown by red regions and have electron-accepting properties. Quercetin (A)'s electronic delocalization spreads across its aromatic rings, distributing both HOMO and LUMO orbitals.

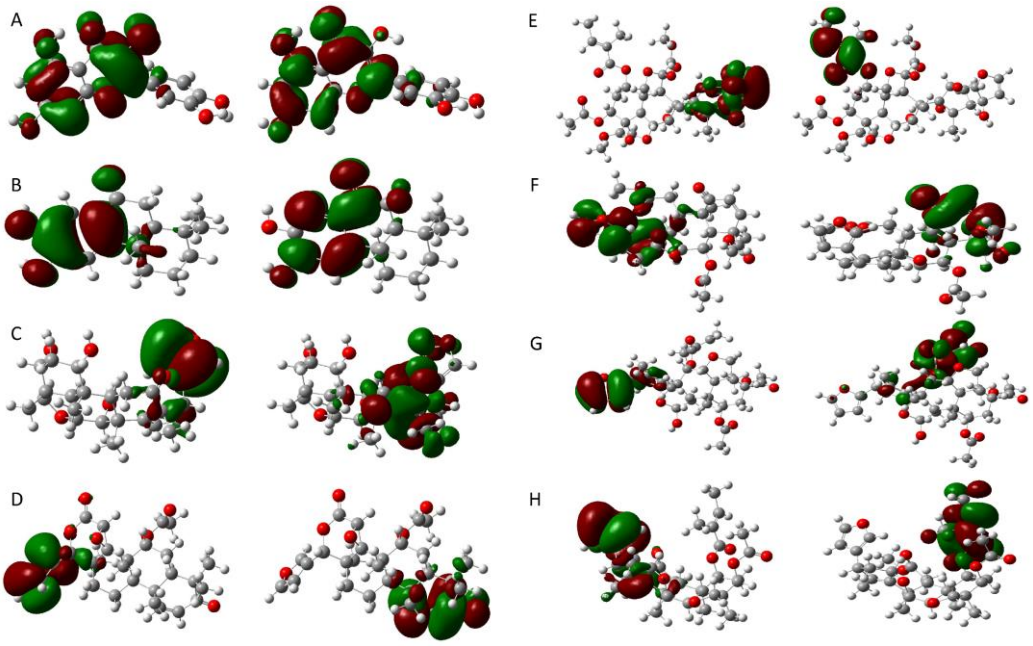

Figure 2. Molecular docking interactions of neem-derived ligands with the FTO protein. (A–C) Three-dimensional representation of the FTO protein bound with selected ligands: **(A)** Quercetin; **(B)** Nimbidol; **(C)** Gedunin, showing their positioning within the active site. Protein secondary structures are highlighted with α-helices (red), β-sheets (cyan), and loops (grey). (D–F) Two-dimensional interaction maps for the corresponding ligands: **(D)** Quercetin; **(E)** Nimbidol; **(F)** Gedunin, illustrating key hydrogen bonds, hydrophobic interactions, and polar contacts with active site residues. Interacting amino acids are color-coded to emphasize their nature and roles in stabilizing the ligand-protein complexes.

This makes it possible for the compound to bind tightly to the FTO protein. Nimbidol (B) and Nimbidin (C) are mainly found in certain functional group areas, which makes it easier for them to communicate selectively. Gedunin (D) and Azadirachtin (E) have complex electron distribution patterns because their large molecular structures suggest moderate binding affinity.

The HOMO-LUMO parts of Nimbin (F), Nimbolinin (G), and Salannin (H) are spread out in different functional groups, which could change how they respond chemically and how they behave. The HOMO-LUMO gap, the energy difference between these two orbitals in comparison with the cocrystallized ligand, is an important indicator of a molecule's chemical reactivity and stability. Visualizations of the molecules' HOMO-LUMO gaps show differences in the ligands' stability and reactivity [49]. This is because smaller gaps connect to higher reactivity. Scientists use orbital images to understand better the electronic factors that affect binding affinity and to explain why molecular docking and free-energy binding tests yield different results.

3.4. Molecular docking.

Table 3 presents how compounds from neem interact with the FTO protein so that researchers can determine how well they can bind and block. Quercetin and FTO have a strong interaction (-7.80 kcal/mol), which occurs through hydrogen bonds and hydrophobic binding patterns in the active site. According to the results, Nimbidol has a strong binding affinity of -7.70 kcal/mol, and Nimbidin has a similar amount of affinity at -7.50 kcal/mol. This suggests that they could be used as strong binders. Gedunin has a strong binding energy of -7.40 kcal/mol, which makes it a good candidate for inhibiting FTO.

Table 3. Binding affinities of neem-derived ligands with the FTO protein. The table lists the binding affinities (in kcal/mol) of the neem-derived compounds as predicted by molecular docking using AutoDock Vina.

S.No	Ligand	Binding affinity (Kcal/mol)
1	Quercetin	-7.80
3	Nimbidol	-7.70
3	Nimbidin	-7.50
4	Gedunin	-7.40
5	Azadirachtin	-5.40
6	Nimbin	-5.00
7	Nimbolinin	-5.00
8	Salannin	-4.40

Azadirachtin (-5.40 kcal/mol), Nimbin (-5.00 kcal/mol), Nimbolinin (-5.00 kcal/mol), and Salannin (-4.40 kcal/mol) have weaker binding affinities than the others. This could be because their interaction doesn't favor fitting well with the FTO binding pocket. Because these compounds are very big and have many different parts, they have lower binding affinities. The binding affinity measurements show that Quercetin, Nimbidol, Nimbidin, and Gedunin have a lot of promise for further research.

Figure 3 shows Quercetin, Nimbidol, and Gedunin, all ligands produced from neem, docking with the FTO protein at the atomic level. This shows how they bind and interact with each other. The active site of the FTO protein can accept all ligands, as shown in Figures A–C. These ligands link with important residues that are needed for the enzyme to work. The way Quercetin (A) binds to the pocket is more stable than the ways Nimbidol (B) and Gedunin (C), even though both ligands are in the right place to bind. This is due to quercetin forming stronger, more stable interactions with key active-site residues of the FTO protein. The two-dimensional interaction maps (D–F) are used to analyze the ligand-protein interaction

thoroughly. Quercetin (D) binds to its target by forming hydrogen bonds and hydrophobic contacts with HIS320, ARG316, and LEU203 residues. Nimbidol (E) is stable because it interacts with SER229 and VAL228 residues in polar and hydrophobic environments, even though it doesn't have many hydrogen bonds. Gedunin (F) binds to MET326 and LEU319 through hydrophobic and van der Waals forces.

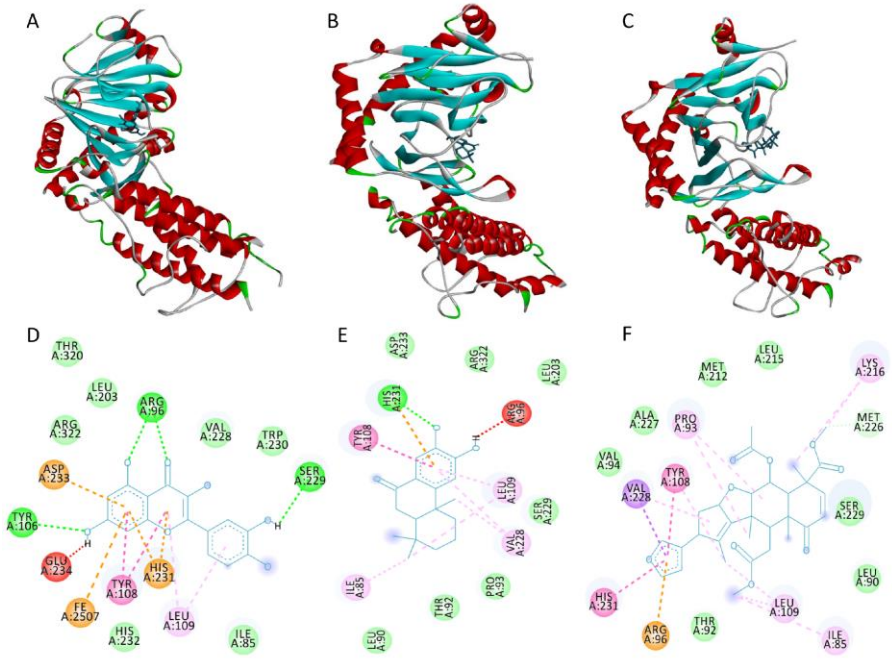

Figure 3. Visualization of HOMO and LUMO orbitals for neem-derived ligands. (A–H) HOMO (green) and LUMO (red) orbitals of neem-derived ligands: **(A)** Quercetin; **(B)** Nimbidol; **(C)** Nimbidin; **(D)** Gedunin; **(E)** Azadirachtin; **(F)** Nimbin; **(G)** Nimbolinin; **(H)** Salannin. The orbital distributions provide insights into the electron density and potential electrophilic and nucleophilic reactivity regions, which are critical for ligand interaction with the FTO protein.

3.5. Binding free energy of complexes.

Table 4 presents the binding free energy describing the stability of the FTO protein-ligand complex formed with compounds derived from neem. It takes -45.749 kcal/mol of quercetin to bind something because its van der Waals energy (-34.798 kcal/mol) and Coulombic energy (-10.951 kcal/mol) make strong non-covalent interactions and electrostatic forces happen. It takes -41.311 kcal/mol and -40.357 kcal/mol for Nimbidin and Gedunin to bind to each other because their van der Waals and Coulombic interactions are equal. The binding energies of Nimbidol and Azadirachtin are -31.841 kcal/mol and -33.152 kcal/mol, respectively.

Table 4. Binding free energy components for neem-derived ligands interacting with the FTO protein. The table presents the energy components, including van der Waals energy (evdw), Coulombic energy (ecoul), total model energy (emodel), binding energy (energy), and internal energy (einternal) for ligands Quercetin, Nimbidol, Nimbidin, Gedunin, and Azadirachtin.

S.No	Ligand	evdw	ecoul	emodel	energy	einternal
1	Quercetin	-34.798	-10.951	-66.499	-45.749	2.498
3	Nimbidol	-27.95	-3.891	-43.269	-31.841	0.506
3	Nimbidin	-33.807	-7.504	-63.272	-41.311	1.548
4	Gedunin	-35.691	-4.666	-49.383	-40.357	2.312
5	Azadirachtin	-24.927	-8.225	-41.255	-33.152	1.557

However, these ligands have strong van der Waals interactions. Free energy calculations show how ligand size, molecular shape, and functional group chemistry affect binding affinity [50]. Quercetin is the most effective compound because it has good van der Waals interactions combined with Coulombic forces.

4. Conclusions

The current research positions compounds extracted from neem as an essential resource for inhibiting FTO inhibition while establishing crucial features of targeting RNA demethylation pathways for future therapeutic development. The combination of computational approaches with natural product analysis provides an economical approach to drug development, offering novel solutions to metabolic diseases and cancers that afflict populations worldwide. While these computational approaches provide a valuable starting point for drug discovery, we recognize that experimental studies are essential to validate the therapeutic potential of the identified neem-derived compounds targeting FTO.

Author Contributions

Investigation, K.M.S. and T.A.; Conceptualization, S.S. and T.A.; Methodology, C.S.S. and R.S.; Data curation M.A. and N.B.; Formal analysis, S.S. and T.A.; Validation, K.M.S. and T.A.; Visualization, C.S.S. and R.S.; Writing – original draft, S.S.; Writing – review & editing, K.M.S. and T.A. All authors have read and agreed to the published version of the manuscript.

Institutional Review Board Statement

Not applicable.

Informed Consent Statement

Not applicable.

Data Availability Statement

Data supporting the findings of this study are available upon reasonable request from the corresponding author.

Funding

This research received no external funding.

Acknowledgments

Declared none.

Conflicts of Interest

The authors declare no conflict of interest.

References

1. Zhang, H.; Zhou, X.-D.; Shapiro, M.D.; Lip, G.Y.; Tilg, H.; Valenti, L.; Somers, V.K.; Byrne, C.D.; Targher, G.; Yang, W. Global burden of metabolic diseases, 1990–2021. *Metabolism* **2024**, *160*, 155999,

https://doi.org/10.1016/j.metabol.2024.155999.
2. Neeland, I.J.; Lim, S.; Tchernof, A.; Gastaldelli, A.; Rangaswami, J.; Ndumele, C.E.; Powell-Wiley, T.M.; Després, J.-P. Metabolic Syndrome. *Nat. Rev. Dis. Prim.* **2024**, *10*, 77, https://doi.org/10.1038/s41572-024-00563-5.
3. Dama, A.; Shpati, K.; Daliu, P.; Dumur, S.; Gorica, E.; Santini, A. Targeting Metabolic Diseases: The Role of Nutraceuticals in Modulating Oxidative Stress and Inflammation. *Nutrients* **2024**, *16*, 507, https://doi.org/10.3390/nu16040507.
4. Klement, R.J. Cancer as a Global Health Crisis with Deep Evolutionary Roots. *Glob. Transitions* **2024**, *6*, 45–65, https://doi.org/10.1016/j.glt.2024.01.001.
5. Sundaram, K.K.M.; Bupesh, G.; Saravanan, K.M. Instrumentals behind Embryo and Cancer: A Platform for Prospective Future in Cancer Research. *AIMS Mol. Sci.* **2022**, *9*, 25–45, https://doi.org/10.3934/molsci.2022002.
6. Bavaharini, R.; Somala, C.S.; Saravanan, K.M.; Anand, T. Neurogranin in Alzheimer's Disease: Roles in Synaptic Function, Pathology, and Potential as a Diagnostic Biomarker. *AIMS Mol. Sci.* **2024**, *11*, 330–350, https://doi.org/10.3934/molsci.2024020.
7. Huang, C.; Chen, W.; Wang, X. Studies on the Fat Mass and Obesity-Associated (FTO) Gene and Its Impact on Obesity-Associated Diseases. *Genes Dis.* **2023**, *10*, 2351–2365, https://doi.org/10.1016/j.gendis.2022.04.014.
8. Somala, C.S.; Sathyapriya, S.; Bharathkumar, N.; Anand, T.; Mathangi, D.C.; Saravanan, K.M. Therapeutic Potential of FTO Demethylase in Metabolism and Disease Pathways. *Protein J.* **2025**, *44*, 21–34, https://doi.org/10.1007/s10930-025-10250-3.
9. Azzam, S.K.; Alsafar, H.; Sajini, A.A. FTO M6A Demethylase in Obesity and Cancer: Implications and Underlying Molecular Mechanisms. *Int. J. Mol. Sci.* **2022**, *23*, 3800, https://doi.org/10.3390/ijms23073800.
10. Abdollahi, S.; Hasanpour Ardekanizadeh, N.; Poorhosseini, S.M.; Gholamalizadeh, M.; Roumi, Z.; Goodarzi, M.O.; Doaei, S. Unraveling the Complex Interactions between the Fat Mass and Obesity-Associated (FTO) Gene, Lifestyle, and Cancer. *Adv. Nutr.* **2022**, *13*, 2406–2419, https://doi.org/10.1093/advances/nmac101.
11. Ren, C.; Cao, Z.; Liu, Y.; Wang, R.; Lin, C.; Wang, Z. Medicinal Chemistry Aspects of Fat Mass and Obesity Associated Protein: Structure, Function and Inhibitors. *Future Med. Chem.* **2024**, *16*, 1705–1726, https://doi.org/10.1080/17568919.2024.2380245.
12. Balaji, A.; Bhuvaneswari, S.; Raj, L.S.; Bupesh, G.; Meenakshisundaram, K.K.; Saravanan, K.M. A Review on the Potential Species of the Zingiberaceae Family with Anti-Viral Efficacy Towards Enveloped Viruses. *J. Pure Appl. Microbiol.* **2022**, *16*, 796–813, https://doi.org/10.22207/JPAM.16.2.35.
13. Chaachouay, N.; Zidane, L. Plant-Derived Natural Products: A Source for Drug Discovery and Development. *Drugs Drug Candidates* **2024**, *3*, 184–207, https://doi.org/10.3390/ddc3010011.
14. Vitale, G.A.; Geibel, C.; Minda, V.; Wang, M.; Aron, A.T.; Petras, D. Connecting Metabolome and Phenotype: Recent Advances in Functional Metabolomics Tools for the Identification of Bioactive Natural Products. *Nat. Prod. Rep.* **2024**, *41*, 885–904, https://doi.org/10.1039/D3NP00050H.
15. Senthil, R.; Archunan, G.; Vithya, D.; Saravanan, K.M. Hexadecanoic Acid Analogs as Potential CviR-Mediated Quorum Sensing Inhibitors in Chromobacterium Violaceum : An *in silico* Study. *J. Biomol. Struct. Dyn.* **2025**, *43*, 3635–3644, https://doi.org/10.1080/07391102.2023.2299945.
16. Batra, N.; Kumar, V.; Nambiar, R.; De Souza, C.; Yuen, A.; Le, U.; Verma, R.; Ghosh, P.; Vinall, R. Exploring the Therapeutic Potential of Neem (Azadirachta Indica) for the Treatment of Prostate Cancer: A Literature Review. *Ann. Transl. Med.* **2022**, *10*, 754, https://doi.org/10.21037/atm-22-94.
17. Wylie, M.R.; Merrell, D.S. The Antimicrobial Potential of the Neem Tree Azadirachta Indica. *Front. Pharmacol.* **2022**, *13*, 891535, https://doi.org/10.3389/fphar.2022.891535.
18. Mayuri, K.; Varalakshmi, D.; Tharaheswari, M.; Somala, C.S.; Priya, S.S.; Bharathkumar, N.; Senthil, R.; Kushwah, R.B.S.; Vickram, S.; Anand, T. Identifying Potent Fat Mass and Obesity-Associated Protein Inhibitors Using Deep Learning-Based Hybrid Procedures. *BioMedInformatics* **2024**, *4*, 347-359, https://doi.org/10.3390/biomedinformatics4010020.
19. Patel, S.M.; Nagulapalli Venkata, K.C.; Bhattacharyya, P.; Sethi, G.; Bishayee, A. Potential of Neem (Azadirachta Indica L.) for Prevention and Treatment of Oncologic Diseases. *Semin. Cancer Biol.* **2016**, *40–41*, 100–115, https://doi.org/10.1016/j.semcancer.2016.03.002.
20. Han, Z.; Niu, T.; Chang, J.; Lei, X.; Zhao, M.; Wang, Q.; Cheng, W.; Wang, J.; Feng, Y.; Chai, J. Crystal Structure of the FTO Protein Reveals Basis for Its Substrate Specificity. *Nature* **2010**, *464*, 1205–1209,

https://doi.org/10.1038/nature08921.
21. Shishodia, S.; Demetriades, M.; Zhang, D.; Tam, N.Y.; Maheswaran, P.; Clunie-O'Connor, C.; Tumber, A.; Leung, I.K.; Ng, Y.M.; Leissing, T.M. Structure-based design of selective fat mass and obesity associated protein (FTO) inhibitors. *J. Med. Chem.* **2021**, *64*, 16609-16625, https://doi.org/10.1021/acs.jmedchem.1c01204.
22. Sarah, R.; Tabassum, B.; Idrees, N.; Hussain, M.K. Bio-active Compounds Isolated from Neem Tree and Their Applications. In Natural Bio-active Compounds: Volume 1: Production and Applications, Akhtar, M.S., Swamy, M.K., Sinniah, U.R., Eds.; Springer Singapore: Singapore, **2019**; pp. 509-528, https://doi.org/10.1007/978-981-13-7154-7_17.
23. Alzohairy, M.A. Therapeutics Role of Azadirachta Indica (Neem) and Their Active Constituents in Diseases Prevention and Treatment. *Evidence-Based Complement. Altern. Med.* **2016**, *2016*, 7382506, https://doi.org/10.1155/2016/7382506.
24. Islas, J.F.; Acosta, E.; G-Buentello, Z.; Delgado-Gallegos, J.L.; Moreno-Treviño, M.G.; Escalante, B.; Moreno-Cuevas, J.E. An Overview of Neem (Azadirachta Indica) and Its Potential Impact on Health. *J. Funct. Foods* **2020**, *74*, 104171, https://doi.org/10.1016/j.jff.2020.104171.
25. Subramani, R.; Gonzalez, E.; Nandy, S.B.; Arumugam, A.; Camacho, F.; Medel, J.; Alabi, D.; Lakshmanaswamy, R. Gedunin Inhibits Pancreatic Cancer by Altering Sonic Hedgehog Signaling Pathway. *Oncotarget* **2017**, *8*, 10891–10904, https://doi.org/10.18632/oncotarget.8055.
26. M. Saravanan, K.; Selvaraj, S. Search for Identical Octapeptides in Unrelated Proteins: Structural Plasticity Revisited. *Pept. Sci.* **2012**, *98*, 11–26, https://doi.org/10.1002/bip.21676.
27. Saravanan, K.M.; Balasubramanian, H.; Nallusamy, S.; Samuel, S. Sequence and Structural Analysis of Two Designed Proteins with 88% Identity Adopting Different Folds. *Protein Eng. Des. Sel.* **2010**, *23*, 911–918, https://doi.org/10.1093/protein/gzq070.
28. Andersa, K.N.; Tamiru, M.; Teka, T.A.; Ali, I.M.; Chane, K.T.; Regasa, T.K.; Ahmed, E.H. Proximate Composition, Some Phytochemical Constituents, Potential Uses, and Safety of Neem Leaf Flour: A Review. *Food Sci. Nutr.* **2024**, *12*, 6929–6937, https://doi.org/10.1002/fsn3.4336.
29. Sandhir, R.; Khurana, M.; Singhal, N.K. Potential Benefits of Phytochemicals from Azadirachta Indica against Neurological Disorders. *Neurochem. Int.* **2021**, *146*, 105023, https://doi.org/10.1016/j.neuint.2021.105023.
30. Sreeraman, S.; Kannan, P.M.; Singh Kushwah, R.B.; Sundaram, V.; Veluchamy, A.; Thirunavukarasou, A.; Saravanan, M.K. Drug Design and Disease Diagnosis: The Potential of Deep Learning Models in Biology. *Curr. Bioinform.* **2023**, *18*, 208–220, http://dx.doi.org/10.2174/1574893618666230227105703.
31. Berman, H.M.; Westbrook, J.; Feng, Z.; Gilliland, G.; Bhat, T.N.; Weissig, H.; Shindyalov, I.N.; Bourne, P.E. The Protein Data Bank. *Nucleic Acids Res.* **2000**, *28*, 235–242, https://doi.org/10.1093/nar/28.1.235.
32. Goodsell, D.S.; Sanner, M.F.; Olson, A.J.; Forli, S. The AutoDock Suite at 30. *Protein Sci.* **2021**, *30*, 31–43, https://doi.org/10.1002/pro.3934.
33. Johansson, M.U.; Zoete, V.; Michielin, O.; Guex, N. Defining and Searching for Structural Motifs Using DeepView/Swiss-PdbViewer. *BMC Bioinformatics* **2012**, *13*, 173, https://doi.org/10.1186/1471-2105-13-173.
34. Sayers, E.W.; Beck, J.; Bolton, E.E.; Brister, J.R.; Chan, J.; Comeau, D.C.; Connor, R.; DiCuccio, M.; Farrell, C.M.; Feldgarden, M. Database resources of the national center for biotechnology information. *Nucleic acids research* **2024**, *52*, D33-D43, https://doi.org/10.1093/nar/gkad1044.
35. Kim, S.; Thiessen, P.A.; Bolton, E.E.; Chen, J.; Fu, G.; Gindulyte, A.; Han, L.; He, J.; He, S.; Shoemaker, B.A.; Wang, J.; Yu, B.; Zhang, J.; Bryant, H.S. PubChem substance and compound databases. *Nucleic acids research* **2016**, *44*, D1202-D1213, https://doi.org/10.1093/nar/gkv951.
36. O'Boyle, N.M.; Banck, M.; James, C.A.; Morley, C.; Vandermeersch, T.; Hutchison, G.R. Open Babel: An Open Chemical Toolbox. *J. Cheminform.* **2011**, *3*, 33, https://doi.org/10.1186/1758-2946-3-33.
37. Daina, A.; Michielin, O.; Zoete, V. SwissADME: A Free Web Tool to Evaluate Pharmacokinetics, Drug-Likeness and Medicinal Chemistry Friendliness of Small Molecules. *Sci. Rep.* **2017**, *7*, 42717, https://doi.org/10.1038/srep42717.
38. Hanwell, M.D.; Curtis, D.E.; Lonie, D.C.; Vandermeersch, T.; Zurek, E.; Hutchison, G.R. Avogadro: An Advanced Semantic Chemical Editor, Visualization, and Analysis Platform. *J. Cheminform.* **2012**, *4*, 17, https://doi.org/10.1186/1758-2946-4-17.
39. Trott, O.; Olson, A.J. AutoDock Vina: Improving the Speed and Accuracy of Docking with a New Scoring Function, Efficient Optimization, and Multithreading. *J. Comput. Chem.* **2010**, *31*, 455–461,

https://doi.org/10.1002/jcc.21334.
40. Pettersen, E.F.; Goddard, T.D.; Huang, C.C.; Couch, G.S.; Greenblatt, D.M.; Meng, E.C.; Ferrin, T.E. UCSF Chimera--a Visualization System for Exploratory Research and Analysis. *J. Comput. Chem.* **2004**, *25*, 1605–1612, https://doi.org/10.1002/jcc.20084.
41. Schrödinger PyMOL, Molecular Visualization System. Available online: https://pymol.org (accessed on 15 January 2025).
42. Kumari, R.; Kumar, R.; Lynn, A. G_mmpbsa—A GROMACS Tool for High-Throughput MM-PBSA Calculations. *J. Chem. Inf. Model.* **2014**, *54*, 1951–1962, https://doi.org/10.1021/ci500020m.
43. Abraham, M.J.; Murtola, T.; Schulz, R.; Páll, S.; Smith, J.C.; Hess, B.; Lindahl, E. GROMACS: High Performance Molecular Simulations through Multi-Level Parallelism from Laptops to Supercomputers. *SoftwareX* **2015**, *1–2*, 19–25, https://doi.org/10.1016/j.softx.2015.06.001.
44. Jorgensen, W.L.; Chandrasekhar, J.; Madura, J.D.; Impey, R.W.; Klein, M.L. Comparison of Simple Potential Functions for Simulating Liquid Water. *J. Chem. Phys.* **1983**, *79*, 926–935, https://doi.org/10.1063/1.445869.
45. Harihar, B.; Saravanan, K.M.; Gromiha, M.M.; Selvaraj, S. Importance of Inter-Residue Contacts for Understanding Protein Folding and Unfolding Rates, Remote Homology, and Drug Design. *Mol. Biotechnol.* **2025**, *67*, 862–884, https://doi.org/10.1007/s12033-024-01119-4.
46. Lipinski, C. Lipinski, C.A. Lead- and Drug-like Compounds: The Rule-of-Five Revolution. Drug Discov. Today Technol. 1, 337-341. *Drug Discov. Today Technol.* **2004**, *1*, 337–341, https://doi.org/10.1016/j.ddtec.2004.11.007.
47. Saravanan, K.M.; Wan, J.-F.; Dai, L.; Zhang, J.; Zhang, J.Z.H.; Zhang, H. A Deep Learning Based Multi-Model Approach for Predicting Drug-like Chemical Compound's Toxicity. *Methods* **2024**, *226*, 164–175, https://doi.org/10.1016/j.ymeth.2024.04.020.
48. Zhang, X.; Wei, L.-H.; Wang, Y.; Xiao, Y.; Liu, J.; Zhang, W.; Yan, N.; Amu, G.; Tang, X.; Zhang, L. Structural insights into FTO's catalytic mechanism for the demethylation of multiple RNA substrates. *Proc. Natl. Acad. Sci. U.S.A.* **2019**, *116*, 2919-2924, https://doi.org/10.1073/pnas.1820574116.
49. Senthil, R.; Meenakshi Sundaram, K.K.; Bupesh, G.; Usha, S.; Saravanan, K.M. Identification of Oxazolo[4,5-g]Quinazolin-2(1H)-One Derivatives as EGFR Inhibitors for Cancer Prevention. *Asian Pacific J. Cancer Prev.* **2022**, *23*, 1687–1697, https://doi.org/10.31557/APJCP.2022.23.5.1687.
50. Saravanan, K.M.; Zhang, H.; Senthil, R.; Vijayakumar, K.K.; Sounderrajan, V.; Wei, Y.; Shakila, H. Structural Basis for the Inhibition of SARS-CoV2 Main Protease by Indian Medicinal Plant-Derived Antiviral Compounds. *J. Biomol. Struct. Dyn.* **2022**, *40*, 1970–1978, https://doi.org/10.1080/07391102.2020.1834457.

Publisher's Note & Disclaimer